Variation of Charge Dynamics in the Course of Metal-Insulator Transition for Pyrochlore-Type $Nd_2Ir_2O_7$

K. Ueda,[1] J. Fujioka,[1] Y. Takahashi,[1] T. Suzuki,[2] S. Ishiwata,[1] Y. Taguchi,[2] and Y. Tokura[1,2]

[1]*Department of Applied Physics and Quantum Phase Electronics Center, University of Tokyo, Tokyo 113-8656, Japan*

[2]*Cross-Correlated Materials Research Group (CMRG) and Correlated Electron Research Group (CERG), RIKEN Advanced Science Institute (ASI), Wako 351-0198, Japan*

(Received 12 June 2012; published 27 September 2012)

We have spectroscopically investigated the thermally and doping-induced metal-insulator transitions for pyrochlore-type $Nd_2Ir_2O_7$ as well as its Rh-doped analogs $Nd_2(Ir_{1-x}Rh_x)_2O_7$, where the spin-orbit interaction as well as the electron correlation is effectively tuned by the doping level (x). The charge dynamics dramatically changes on an energy scale of 1 eV in the course of thermally and doping-induced metal-insulator transitions, while the insulating ground state shows a small but well-defined charge gap of 45 meV. Anomalous doping variation of the low-energy (< 0.3 eV) optical-conductivity spectra at the ground state can be interpreted in terms of the phase changes among the narrow-gap Mott insulator, Weyl semimetal, and correlated metal.

DOI: 10.1103/PhysRevLett.109.136402 PACS numbers: 71.30.+h, 72.80.Ga, 78.20.−e, 78.30.−j

The electron correlation effect in $3d$- or $4d$-transition metal oxides has received an enormous amount of attention, since it often produces a variety of emergent phenomena such as metal-insulator transition (MIT), high-T_C superconductivity, and colossal magnetoresistance [1]. In contrast, the $5d$-transition metal oxides have been believed to be categorized as weakly electron correlated systems due to their larger effective band width. Recent extensive studies, however, have shown that the strong spin-orbit interaction (SOI) inherent in heavy $5d$-transition metal ions effectively enhances the electron correlation via reshuffling of the $5d$-band manifold, which provides a new platform for emergent electronic or magnetic collective phenomena [2–4].

Among them, the pyrochlore-type $R_2Ir_2O_7$ (R is the rare-earth elements) has been attracting much attention for the possible formation of topologically nontrivial electronic structures in the presence of both strong SOI and electron correlation, such as the topological Mott insulator, zero-gap semimetal with Weyl points (Weyl semimetal), and axion insulator [4–9]. For $R_2Ir_2O_7$, both R- and Ir-sublattices form networks of corner-sharing tetrahedra and the nominal electronic configuration of Ir^{4+} is $5d\ t_{2g}^5$. The strong SOI lifts the degeneracy of $5d\ t_{2g}$ manifold into the lower-lying $J_{\mathrm{eff}} = 3/2$ quadruplet and higher-lying $J_{\mathrm{eff}} = 1/2$ doublet bands. The former is fully occupied and energetically well separated from the latter, whereas the latter is half-filled and plays a major role in the electronic or magnetic properties [4–6].

As shown in Figs. 1(a) and 1(b), $Nd_2Ir_2O_7$ undergoes a thermally induced MIT concomitantly with the magnetic ordering at $T_N = 32$ K, where the resistivity dramatically increases and magnetization exhibits an onset in the field cooling (FC) process [10]. On the basis of neutron diffraction experiments, Tomiyasu *et al.* argued that the magnetic transition at T_N corresponds to the ordering of Ir-$5d$ moments in the all-in all-out type configuration, where all the Ir-$5d$ moments are pointing toward or outward from the center of each tetrahedron [11]. By changing R from Nd to Ho, T_N monotonically increases up to 141 K, and the system becomes a semiconductor below room temperature

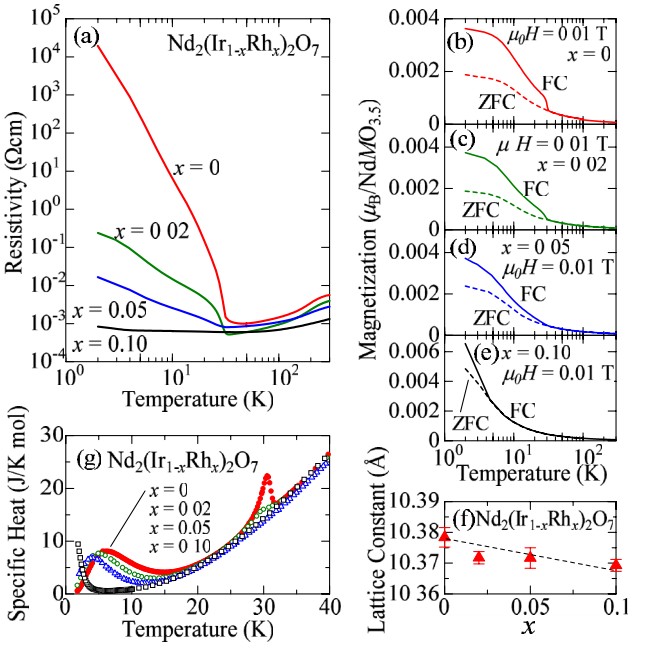

FIG. 1 (color online). The temperature dependence of (a) the resistivity for $Nd_2(Ir_{1-x}Rh_x)_2O_7$ ($x = 0$, 0.02, 0.05, 0.10), the magnetization for (b) $x = 0$, (c) $x = 0.02$, (d) $x = 0.05$, (e) $x = 0.10$ (FC and ZFC denote field cooling and zero field cooling, respectively), (f) the x dependence of lattice constant, and (g) the specific heat for $x = 0$ (●), $x = 0.02$ (○), $x = 0.05$ (△), $x = 0.10$ (□).

[10,12–14], while $Pr_2Ir_2O_7$ is metallic down to 0.3 K and shows no long-range magnetic ordering except for the freezing of Pr-4f or Ir-5d moments at 0.12 K [15]. Despite these experimental investigations on the electronic or magnetic properties for these systems, the origin of MIT has been left elusive.

In this study, we have systematically investigated the evolution of the charge dynamics as well as the transport, magnetic, and thermal properties in the course of MIT for the pyrochlore-type $Nd_2Ir_2O_7$ and its Rh-doped analogs $Nd_2(Ir_{1-x}Rh_x)_2O_7$. Rh doping is done to finely tune the interplay between the SOI and the electron correlation, and hence to drive the insulator-metal transition at the ground state. The observed features suggest that the MITs for the present system can be viewed as the phase changes among the correlated metal, the Weyl semimetal, and the narrow gap Mott insulator, as characterized by the strong SOI and electron correlation.

The high-quality polycrystalline samples of $Nd_2(Ir_{1-x}Rh_x)_2O_7$ with $x = 0$, 0.02, 0.05, and 0.10 were prepared by a solid-state reaction under high pressure (3 GPa and 1200 °C). The dense and hard samples with least grain-boundary effect as prepared by the high-pressure method are particularly suitable for the optical reflectance and transport measurements. We have confirmed by powder x-ray diffraction that all the samples imply no detectable impurity phase, and the lattice constant of the Rh-doped compounds satisfies Vegard's law, as shown in Fig. 1(f). The resistivity, specific heat, and magnetization were measured with the physical property measurement system (Quantum Design). Reflectivity spectra in the temperature range from 5 to 290 K were measured between 0.005 and 5 eV by Fourier transform- and grating-type spectrometers. The spectra above 5 eV were measured at room temperature with the use of synchrotron radiation at UV-SOR, Institute for Molecular Science. The optical conductivity spectra were obtained by Kramers-Kronig (KK) analysis with suitable extrapolation procedures. The optical conductivity spectra below 10 meV were obtained by terahertz (THz) time-domain spectroscopy (TDS) in a transmission configuration [16] without resorting to KK analysis (for details of the experimental setup for the present THz TDS, see Sec. II Ref. [16]).

The temperature dependence of resistivity for $Nd_2Ir_2O_7$ ($x = 0$) is shown in Fig. 1(a), along with those for $x = 0.02$, 0.05, and 0.10. First, we focus on the MIT in $Nd_2Ir_2O_7$ ($x = 0$). With lowering temperature, the resistivity for $x = 0$ monotonically decreases down to 50 K and then shows a divergent behavior below 30 K. In Fig. 1(b), we show the temperature dependence of magnetization measured by field-cooling (FC) and zero-field-cooling (ZFC) processes. The magnetization curve measured in the FC process shows an upturn at T_N, while that measured in the ZFC process shows no clear anomaly with previous reports [10]. As shown in Fig. 1(g), the ordering of the Ir-5d moment manifests itself as a λ-type peak at T_N in the specific heat curve for $x = 0$. A recent neutron scattering study indicates that the Nd-4f moment starts to order below 15 K [11]. Since the energy of the crystal field (CF) splitting between the ground state and the first excited state is estimated to be 26 meV ($\sim$ 300 K) [11], a broad hump-like structure around 10 K may be attributed not to CF excitation but to the magnetic ordering of Nd-4f moments. We note that the entropy change except the contribution from phonon below 20 K is larger than $R\ln 2$, the value corresponding to the entropy released by the magnetic ordering of Nd-4f moments as observed in spin-ice systems [17]. The excess entropy change may originate from the coupled Ir-5d moments, reflecting the exchange interaction between Nd-4f and Ir-5d moments.

Figure 2(a) displays the optical conductivity spectra for $Nd_2Ir_2O_7$ ($x = 0$) at various temperatures above 50 K as well as at 10 K. At 290 K, a broad absorption band is observed around 1 eV, as shown in the inset to Fig. 2(a). Since the optical conductivity spectra above 1 eV show minimal temperature dependence, we henceforth focus on the low energy range below 1 eV. At room temperature, the spectral shape below 0.5 eV is fairly flat except for the sharp peaks due to the optical phonons below 0.08 eV,

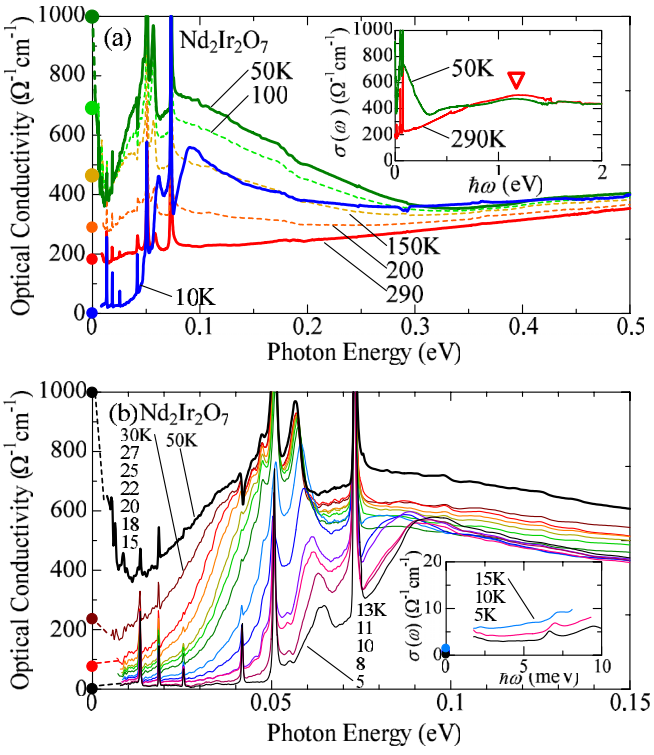

FIG. 2 (color online). (a) Optical conductivity spectra at various temperatures for $Nd_2Ir_2O_7$. The filled circles denote dc conductivities. The inset shows the spectra at 290 K and 50 K up to 2 eV. The triangle indicates the absorption band around 1 eV. (b) Optical conductivity spectra below 50 K. The inset show the magnified view of the spectra in the far-infrared region as deduced by time-domain terahertz spectroscopy.

suggesting that incoherent charge dynamics governs the dc charge transport as well. A hump-like structure appears around 0.06 eV, whose spectral weight is markedly enhanced as the temperature decreases, together with a sharp Drude peak below 0.01 eV. Figure 2(b) shows the low-energy region of optical conductivity spectra below 50 K. As the temperature is further lowered, the hump-like structure becomes sharpened, decreasing the spectral intensity, and turns into a gapped absorption peak centered at 0.1 eV. Some sharp phonon profiles are subject to the Fano resonance effect due to the overlapping electronic background, yet no major change, e.g., splitting of the mode, is discerned, indicating that the lattice symmetry is not changed upon MIT. At 5 K, the optical conductivity below 0.05 eV is too small to be precisely estimated by measurement of the reflectivity spectra. The inset to Fig. 2(b) shows the optical conductivity spectra deduced by the THz TDS in transmission configuration. The optical conductivity below 5 meV is extremely small (less than 5 $\Omega^{-1}\,\mathrm{cm}^{-1}$) below 10 K, allowing us to conclude the full opening of the charge gap. The charge gap energy, which is defined as an onset energy of the steeply rising part of the optical conductivity, is estimated to be 45 meV at 5 K.

To quantitatively characterize the temperature dependence of spectral weight, we have calculated the effective number of electrons (N_{eff}), defined as

$$N_{\mathrm{eff}}(\hbar\omega_c) = \frac{2m_0 V}{\pi e^2}\int_0^{\omega_c}\sigma(\omega)d\omega. \qquad (1)$$

Here m_0, V, and ω_c are the free-electron mass, cell volume, and cutoff energy, respectively. We plotted the temperature dependence of $N_{\mathrm{eff}}(\hbar\omega_c = 50\ \mathrm{meV})$ and $N_{\mathrm{eff}}(\hbar\omega_c = 300\ \mathrm{meV})$ in Figs. 3(a) and 3(b), respectively. Both $N_{\mathrm{eff}}(\hbar\omega_c = 50\ \mathrm{meV})$ and $N_{\mathrm{eff}}(\hbar\omega_c = 300\ \mathrm{meV})$ increase when cooled from 300 K to 50 K, but decrease below T_{N} in accord with the charge gap opening.

Important insight into the origin of the insulating state is provided by the effective tuning of the SOI via Rh-ion doping. Since the nominal electronic configuration of $\mathrm{Rh}^{4+}(4dt_{2g}^5)$ is isoelectronic to that of $\mathrm{Ir}^{4+}(5dt_{2g}^5)$, Rh-ion doping would effectively reduce the strength of SOI in the amalgamated 4d-5d band scheme, keeping the nominal band filling intact [18]. In Fig. 1(a), we show the temperature dependence of resistivity for $\mathrm{Nd}_2(\mathrm{Ir}_{1-x}\mathrm{Rh}_x)_2\mathrm{O}_7$ with $x = 0.02$, 0.05, and 0.10 together with that for $x = 0$. With increasing x, the resistivity at low temperatures dramatically decreases and shows a metallic behavior for $x = 0.10$, apart from the slight upturn below 5 K. As shown in Figs. 1(c)–1(e), the difference in magnetization between the FC and ZFC processes is observed below 30 K for $x = 0.02$ and 0.05, but is no longer clear for $x = 0.10$. The specific heat curves for $x = 0.02$, 0.05, and 0.10 show a broad hump-like structure below 10 K, which shifts to lower temperatures as x increases. This is perhaps because the coupled (all-in all-out) order of the Nd-4f and the Ir-5d moments via the f-d exchange interaction is suppressed with increasing x.

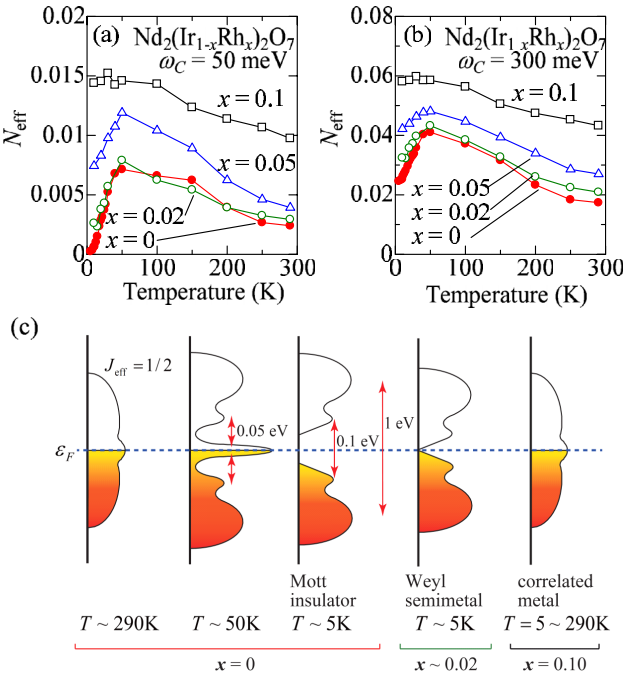

FIG. 3 (color online). Temperature dependence of the effective number of electrons (a) for 50 meV [N_{eff}(50 meV)] and (b) for 300 meV [N_{eff}(300 meV)]. (●: $x = 0$, ○: $x = 0.02$, △: $x = 0.05$ and □: $x = 0.10$). (c) The schematic diagrams for the electronic structure for $x = 0$ at various temperatures as well as those for $x = 0.02$ (Weyl semimetal) and 0.10 (correlated metal) at the ground state ($T \sim 5$ K).

We show the optical conductivity spectra at various temperatures for $x = 0.02$, 0.05, and 0.10 in comparison with those for $x = 0$ in Figs. 4(a)–4(d). The spectra at 290 K are rather flat below 0.1 eV and show a broad absorption band centered at 1 eV, as seen in that for $x = 0$. Below 50 K, as shown in Figs. 4(b) and 4(c), the hump-like structure is discernible at 0.05 eV (0.06 eV) at low temperatures for $x = 0.02$ ($x = 0.05$), as in the case for $x = 0$, while it is not clear apart from the broad Drude peak for $x = 0.10$. We note that the onset of the steeply rising part of optical conductivity continuously shifts to lower energy with increasing x at 5 K, as shown in Fig. 4(d); this indicates the nearly continuous closing of the charge gap in the course of the doping-induced MIT. To quantitatively evaluate the temperature dependence of the spectral weight, we plotted N_{eff} also for $x = 0.02$, 0.05, and 0.10 in comparison with that for $x = 0$ as a function of temperature in Figs. 3(a) and 3(b), respectively. As x increases, the temperature dependence of N_{eff} becomes small, while the low-energy spectral-weight loss is discerned below 50 K for $x = 0.02$ and 0.05, similar to the case of $x = 0$. For $x = 0.10$, however, not only

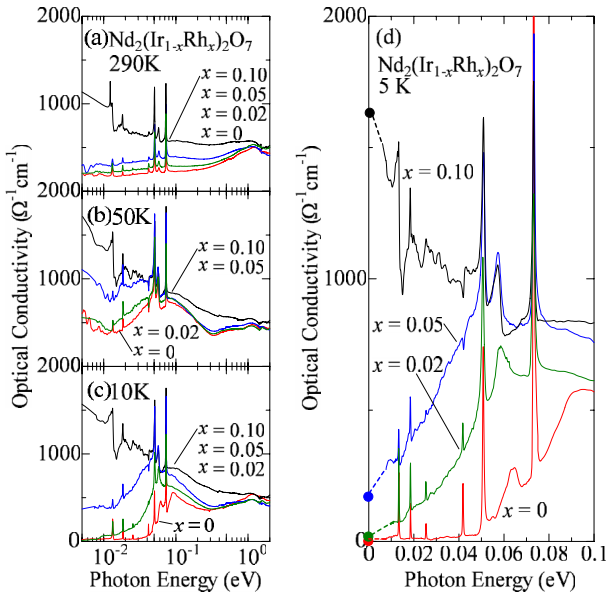

FIG. 4 (color online). Optical conductivity spectra at (a) 290 K, (b) 50 K, (c) 10 K, and (d) 5 K. The red, green, blue, and black line indicates the spectra for $x = 0$, 0.02, 0.05, and 0.10, respectively. The filled circles denote the dc conductivity and the dashed lines are the guide to the eyes.

$N_{\mathrm{eff}}(\omega_c = 50\ \mathrm{meV})$ but also $N_{\mathrm{eff}}(\omega_c = 300\ \mathrm{meV})$ monotonically increase as the temperature decreases, indicating that a change in the charge dynamics on the energy scale of higher than 0.3 eV is determinant to the temperature dependence of dc-charge transport below 300 K. These results suggest that a tuning of the SOI via Rh doping would significantly change the electronic structure near the Fermi level on an energy scale of 1 eV, turning the magnetic Mott insulator into the incoherent paramagnetic metallic one via the semimetallic or zero-gap state.

Several scenarios have been theoretically proposed up to now as the origin of the insulating or semiconducting phase for the present system [4–9]. Wan *et al.* proposed the Weyl semimetal by *ab initio* calculation, which shows linearly dispersing bands with vanishing density of state at Fermi energy [5]. They argue that the Weyl semimetallic phase emerges when the strength of electron correlation (U) is moderate (~ 1.5 eV), and therein the optical conductivity is proportional to photon energy ($\sigma(\omega) \propto \omega$) in the limit of clean systems. This model is not consistent with the clear charge gap discerned at low temperatures for $x = 0$, but is in accord with the features of the optical conductivity spectra for the $x = 0.02$ and 0.05 compounds in which the magnetic order, perhaps all-in all-out, appears to survive at the ground state.

We note that the evolution of charge dynamics upon MITs for the present system is quite unique among the conventional Mott insulators. For example, in V_2O_3, which is known as a prototypical Mott insulator, a large spectral intensity in the low-energy region originating from the Drude response and incoherent charge excitation is nearly completely transferred to the higher energy region upon MIT, and a charge gap with an energy scale of U (~ 1 eV) opens in the Mott insulating phase [1,19,20]. For the present system, on the other hand, the spectral weight in the low-energy region substantially subsists as the absorption band centered at 0.1 eV even in the insulating phase, leading to a small charge gap energy (~ 45 meV), which is further tuned to the zero-gap state by Rh doping (x). Such an evolution of charge dynamics is reminiscent of the phase transition between the Mott insulator and Dirac semimetal predicted for the two-dimensional honeycomb lattice system [21], where the latter phase is characterized by linearly dispersing bands with vanishing density of state at Fermi energy, similarly to the Weyl semimetal. Recent theoretical studies on systems of this model have shown that charge gap opening occurs in a nearly continuous manner upon Mott transition [21]. It is also predicted for the present system that the Weyl semimetallic and Mott insulating phases will compete with each other when the electron correlation strength is effectively tuned (around $U = 1.8$ eV) [5]. It is thus expected that the Mott insulating state in proximity to the Weyl semimetallic state for $x = 0$ turns into the Weyl semimetallic state with dilute Rh doping ($x = 0.02$), and finally into the correlated metal for the heavily Rh-doped system ($x = 0.10$). On the basis of these results, we schematically depict the evolution of the electronic structure upon the thermally and Rh-doping-induced MIT in Fig. 3(c).

In conclusion, we have investigated the evolution of charge dynamics upon metal-insulator transition for the pyrochlore-type $Nd_2(Ir_{1-x}Rh_x)_2O_7$. For $x = 0$, the charge dynamics significantly changes over a wide energy range up to 0.5 eV in the course of the MIT; the spectral weight is accumulated below 0.3 eV with lowering temperature down to the MIT temperature, while a full charge gap with an energy of 45 meV is clearly observed in the insulating ground state. The reduction of the spin-orbit interaction via Rh-ion doping results in the effective reduction of the electron correlation effect and the nearly continuous charge-gap closing, as accompanied by the reconstruction of the electronic structure near the Fermi level on an energy scale of 1 eV. These results can be interpreted as the successive ground-state phase changes among the narrow-gap Mott insulator, Weyl semimetal, and correlated metal, which are all characterized by the interplay between the strong SOI and electron correlation on the pyrochlore lattice.

We thank M. Imada and N. Nagaosa for enlightening discussions. This work was partly supported by Grants-in-Aid for Scientific Research (Grants No. 20340086, No. 23840010, and No. 22014003) from the MEXT of Japan and FIRST Program by the Japan Society for the Promotion of Science (JSPS).

[1] M. Imada, A. Fujimori, and Y. Tokura, Rev. Mod. Phys. **70**, 1039 (1998).
[2] B. J. Kim, H. Ohsumi, T. Komesu, S. Sakai, T. Morita, H. Takagi, and T. Arima, Science **323**, 1329 (2009).
[3] S. J. Moon *et al.*, Phys. Rev. Lett. **101**, 226402 (2008).
[4] D. Pesin and L. Balents, Nature Phys. **6**, 376 (2010).
[5] X. Wan, A. M. Turner, A. Vishwanath, and S. Y. Savrasov, Phys. Rev. B **83**, 205101 (2011).
[6] B. J. Yang and Y. B. Kim, Phys. Rev. B **82**, 085111 (2010).
[7] M. Kurita, Y. Yamaji, and M. Imada, J. Phys. Soc. Jpn. **80**, 044708 (2011).
[8] W. Witczak-Krempa and Y. B. Kim, Phys. Rev. B **85**, 045124 (2012).
[9] M. Kargarian, J. Wen, and G. A. Fiete, Phys. Rev. B **83**, 165112 (2011).
[10] K. Matsuhira, M. Wakeshima, Y. Hinatsu, and S. Takagi, J. Phys. Soc. Jpn. **80**, 094701 (2011).
[11] K. Tomiyasu, K. Matsuhira, K. Iwasa, M. Watahiki, S. Takagi, M. Wakeshima, Y. Hinatsu, M. Yokoyama, K. Ohoyama, and K. Yamada, J. Phys. Soc. Jpn. **81**, 034709 (2012).
[12] D. Yanagishima and Y. Maeno, J. Phys. Soc. Jpn. **70**, 2880 (2001).
[13] N. Taira, M. Wakeshima, and Y. Hinatsu, J. Phys. Condens. Matter **13**, 5527 (2001).
[14] R. S. Singh, V. R. R. Medicherla, K. Maiti, and E. V. Sampathkumaran, Phys. Rev. B **77**, 201102(R) (2008).
[15] S. Nakatsuji, Y. Machida, Y. Maeno, T. Tayama, T. Sakakibara, J. van Duijn, L. Balicas, J. N. Millican, R. T. Macaluso, and J. Y. Chan, Phys. Rev. Lett. **96**, 087204 (2006).
[16] N. Kida, Y. Ikebe, Y. Takahashi, J. P. He, Y. Kaneko, Y. Yamasaki, R. Shimano, T. Arima, N. Nagaosa, and Y. Tokura, Phys. Rev. B **78**, 104414 (2008).
[17] Y. Onose, Y. Taguchi, T. Ito, and Y. Tokura, Phys. Rev. B **70**, 060401 (2004).
[18] J. S. Lee, Y. Krockenberger, K. S. Takahashi, M. Kawasaki, and Y. Tokura, Phys. Rev. B **85**, 035101 (2012).
[19] M. J. Rozenberg, G. Kotliar, H. Kajueter, G. A. Thomas, D. H. Rapkine, J. M. Honig, and P. Metcalf, Phys. Rev. Lett. **75**, 105 (1995).
[20] L. Baldassarre *et al.*, Phys. Rev. B **77**, 113107 (2008).
[21] S. A. Jafari, Eur. Phys. J. B **68**, 537 (2009); A. Liebsch, Phys. Rev. B **83**, 035113 (2011).